The Thermal Sieve: a diffractive baffle that provides thermal isolation of a cryogenic optical system from an ambient temperature collimator

James H. Burge[*] and Dae Wook Kim

College of Optical Sciences
University of Arizona
Tucson, AZ USA 85721

ABSTRACT

We present the thermal sieve, which is a diffractive baffle that provides thermal isolation between an ambient collimator and a cryogenic optical system being measured. The baffle uses several parallel plates with holes in them. The holes are lined up to allow the collimated light to pass, but the view factor for thermal radiation is greatly reduced. A particular design is shown here that allows less than $0.25 \ W/m^2$ thermal transfer and degrades the test wavefront by only 3 nm rms.

Keywords: Space optics, collimator, cryogenic testing

1. INTRODUCTION

Optical imaging systems are being built that operate in cold space or in very cold climates, such as Antarctica. It is seldom practical to test such systems in their final operational environment. Systems that operate at ambient temperatures are commonly tested using collimators that feed the imaging system with light that appears to come from far away. But the thermal gradients caused by exposing a cryogenic system to an ambient temperature collimator will create large distortions and make testing difficult. For cases where the system being tested must operate at cold temperatures, several options available are shown in Table 1.

The difficulty of optical testing for cryogenic systems arises because of the following aspects of the systems:

- The operational systems will have degraded performance at ambient temperatures. They are designed to operate cold.

- The operational systems are sensitive to thermal conditions. Radiation from an ambient temperature object will induce thermal gradients that degrade the system performance.

- The collimators or test optics themselves are sensitive to thermal conditions. Radiation to a cryogenically cooled surface will induce thermal gradients that degrade performance.

- Any test of high performance systems must use optics to create wavefronts that are nearly perfect. Otherwise, errors in the test optics will limit the ability to measure the performance of the imaging system under test.

*jburge@optics.arizona.edu

Table 1. Options available for testing cryogenic optical imaging systems

Concept	Comments
Use a cryogenic collimator 	Cryogenic optics are very expensive and risky. A full aperture cryogenic collimator could cost as much as the system that it is measuring. It would be difficult to verify the performance of the collimator. An alternative is testing with a full aperture autocollimating flat. Control of the figure of the flat at temperature is expensive and risky.[1]
Test through a window 	A large aperture, high quality window is expensive. The window is difficult to calibrate. It is difficult to provide thermal isolation, yet allow light to pass. Most small systems are tested this way.
Subaperture testing + stitching Allows use of smaller window or test system 	Smaller test allows the use of a smaller window, or smaller optics that must operate cold. Multiple overlapping measurements can be "stitched" to provide full aperture data. Data acquisition can be cumbersome. Subject to noise and variations during the testing
Quantify performance by analysis Rely on combination of component testing and modeling	For systems with active controls, a full aperture measurement may not be required.[2]
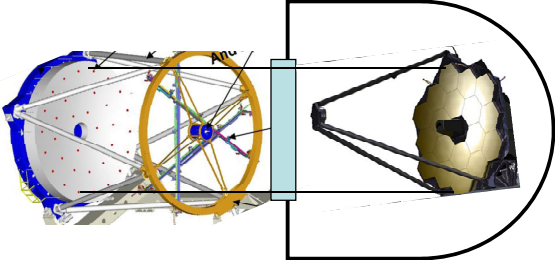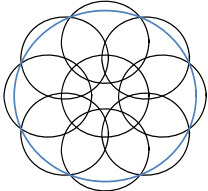
For the ideal case, an ambient temperature collimator, such as LOTIS[3], can be used for measuring a large cryogenic system. This can be accomplished with a thermal sieve that allows the test light to pass, yet limits the heat transfer from radiative coupling. This is accomplished using plates that have holes in them, with the holes lined up to pass the collimated test light, but the holes small enough to limit the view factor for heat transfer.

The thermal sieve (TS) is placed between the collimator and the optical system under test as shown in Fig. 1 (right). There are four major design parameters for a TS; i) N: Number of thermal plates, ii) S: Spacing between the thermal plates, iii) D_{hole}: hole diameter, and iv) I: Interval between holes. The concepts of the thermal sieve, and an example design are provided here, and some engineering details are given in a recent publication from the authors.[4] Much of the material in the current paper is drawn directly from Reference 4.
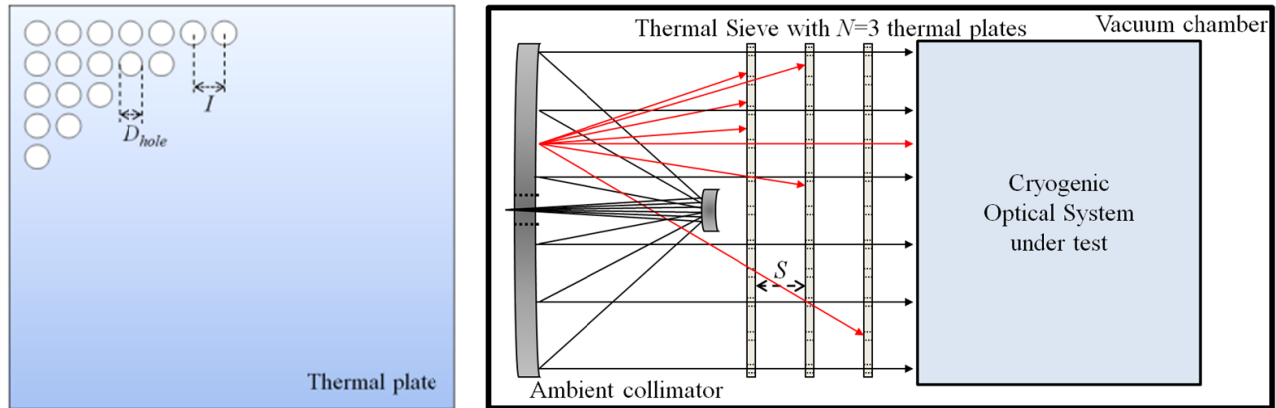
Figure 1. Thermal sieve made of plates with array of holes (left) and a conceptual cryogenic optical testing configuration using TS in a vacuum chamber (right) (Note: The red rays represent the thermal radiation from the collimator, and the black rays represent the collimated test beam.)

A point source projected to infinity by the large collimator provides a collimated test beam (black rays in Fig. 1 (right)). This collimated beam passes through the array of holes in the TS. Because of the diffraction from the array of holes, the test beam has multiple diffraction orders. Those orders represent multiple plane waves with different propagation angles, and the plane waves are fed in to the optical system under test. The collimator can create a small field of view which is passed by the thermal sieve with essentially no degradation. Other orders of diffraction will have a number of defects, most notably chromatic aberration.
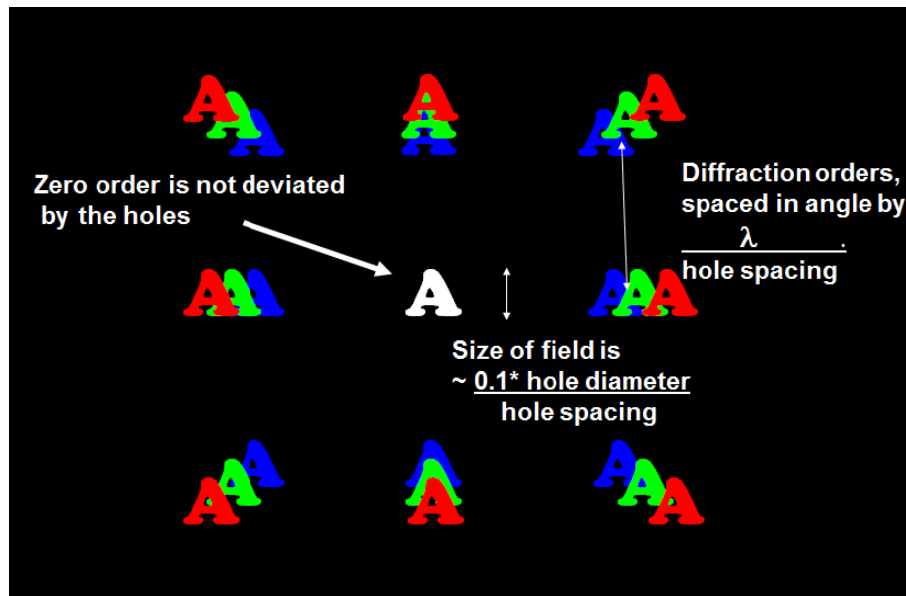
Figure 2. The zero order image through the holes is reduced in brightness due to the thermal sieve, but the image quality is not affected. Higher orders of diffraction will also be present.

The optical performance of the system under test can be measured using standard MTF targets. A more quantitative assessment can be made by using phase diversity methods that provide the wavefront phase error using images through focus. The fact that the zero-order image was created from a set of holes, rather than a continuous wavefront does not change the behavior of the zero order image.

2. THERMAL DESIGN

The radiative heat transfer relationships for a thermal sieve were developed to determine the flow of thermal energy from one space to another. The thermal transfer between the plates is defined by the emissivity and temperature of the plates and the relatively small area encompassed by the holes. The problem is simplified by ignoring edge effects, assuming infinite plates with holes defined only by the fractional area. The collimator and optical system spaces are represented by two blackbodies with their operating temperatures T_H and T_C. The thermal plates are modeled as graybodies with controlled temperatures T_{1-3} and emissivity ε_{1-3} values, corresponding to the 1st, 2nd, and 3rd plates . The emissive power J from these graybodies is given from Stefan-Boltzmann law

$$J = \varepsilon \cdot \sigma \cdot T^4 \ [W/m^2].$$

(Eq. 1)

where ε is the emissivity, σ is the Stefan-Boltzmann constant 5.67×10^{-8} $W/m^2/K^4$, and T is the absolute temperature of the graybody.
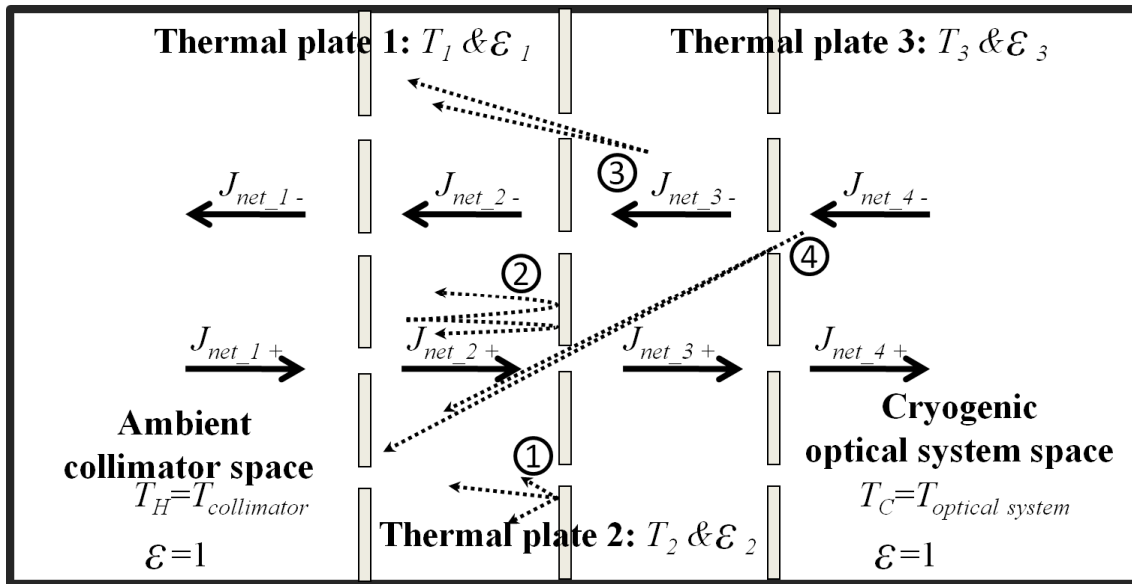
Figure 3. Thermal transfer model with three thermal plates in a vacuum chamber. The solid arrows represent the net directional thermal flux in each space. Also, as an example, four emissive power components contributing to J_{net_2-} are depicted as dotted arrows 1-4. (1) Graybody radiation from the 2nd thermal plate, (2) Reflection of J_{net_2+} by the 2nd thermal plate, (3) Leak of J_{net_3-} through the 2nd plate holes except the power directly passes through the 1st plate holes, and (4) Leak of J_{net_4-} through the 3rd and 2nd plate holes except the power directly passes through the 1st plate holes.

A set of interconnected steady state thermal transfer equations is defined for each space using thermal radiation and geometry. For instance, the net power J_{net_2-} can be found as a sum of the contributions, shown as dotted arrows in Fig. 3. The thermal transfer equation becomes

$$
\begin{aligned}
J_{net\_2-} = {} & \varepsilon_2 \cdot \sigma \cdot T_2^4 \cdot \alpha && : (1)\,in\,Fig.3. \\
& + J_{net\_2+} \cdot (1-\varepsilon_2) \cdot \alpha && : (2)\,in\,Fig.3. \\
& + J_{net\_3-} \cdot \frac{(\pi - \Omega_{eff1})}{\pi} \cdot (1-\alpha) && : (3)\,in\,Fig.3. \\
& + J_{net\_4-} \cdot \frac{(\Omega_{eff1} - \Omega_{eff2})}{\pi} \cdot (1-\alpha) && : (4)\,in\,Fig.3.
\end{aligned}
$$

(Eq. 2)

where the obscuration ratio α of each thermal plate was defined as the ratio of the not-a-hole region area to the whole thermal plate area. Two effective solid angle Ω_{eff1} and Ω_{eff2} represent the sum of solid angles encompassed by the array of holes in the neighboring plate (S away) and the following plate ($2S$ away), respectively. These solid angles are expressed using approximated projected solid angles with $cos^4\theta$ scale factor as

$$\Omega_{eff1} \cong \frac{\pi \cdot (D_{hole}/2)^2}{S^2}(1 + 4\sum_{\substack{n=1\\m=0}}^{\infty}\cos^4\theta) = \frac{\pi \cdot D_{hole}^2}{4S^2}\{1 + 4\sum_{\substack{n=1\\m=0}}^{\infty}(\frac{S}{\sqrt{S^2 + I^2(n^2+m^2)}})^4\}\cdot \quad \text{(Eq. 3)}$$

and

$$\Omega_{eff2} \cong \frac{\pi \cdot (D_{hole}/2)^2}{(2S)^2}(1 + 4\sum_{\substack{n=1\\m=0}}^{\infty}\cos^4\theta) = \frac{\pi \cdot D_{hole}^2}{16S^2}\{1 + 4\sum_{\substack{n=1\\m=0}}^{\infty}(\frac{S}{\sqrt{S^2 + I^2(n^2+m^2)}})^4\}\cdot \quad \text{(Eq. 4)}$$

where θ is the angle shown in Fig. 3. The n and m represent the relative column and row differences between two holes in the thermal plates as depicted in Fig. 3. Infinite number of holes (i.e. infinite n and m) was assumed instead of using the actual number of the holes. This eliminates the geometrical asymmetry problem (e.g. edge effect) for evaluating the effective solid angles not at the center of thermal plate.

A similar analysis was performed for the other spaces for a 3-plate system, resulting in a set of inter-related transfer equations. These are expressed in matrix form as

$$\begin{bmatrix}
1 & 0 & 0 & 0 & 0 & 0 & 0 & 0 \\
(\varepsilon_1-1)\alpha & 1 & 0 & (\alpha-1) & 0 & \Omega_{eff1}(\alpha-1)/\pi & 0 & \Omega_{eff2}(\alpha-1)/\pi \\
(\pi-\Omega_{eff1})(\alpha-1)/\pi & 0 & 1 & (\varepsilon_1-1)\alpha & 0 & 0 & 0 & 0 \\
0 & 0 & (\varepsilon_2-1)\alpha & 1 & 0 & (\pi-\Omega_{eff1})(\alpha-1)/\pi & 0 & (\Omega_{eff1}-\Omega_{eff2})(\alpha-1)/\pi \\
(\Omega_{eff1}-\Omega_{eff2})(\alpha-1)/\pi & 0 & (\pi-\Omega_{eff1})(\alpha-1)/\pi & 0 & 1 & (\varepsilon_2-1)\alpha & 0 & 0 \\
0 & 0 & 0 & 0 & (\varepsilon_3-1)\alpha & 1 & 0 & (\pi-\Omega_{eff1})(\alpha-1)/\pi \\
\Omega_{eff2}(\alpha-1)/\pi & 0 & \Omega_{eff1}(\alpha-1)/\pi & 0 & (\alpha-1) & 0 & 1 & (\varepsilon_3-1)\alpha \\
0 & 0 & 0 & 0 & 0 & 0 & 0 & 1
\end{bmatrix}\begin{bmatrix}
J_{net\_1+} \\
J_{net\_1-} \\
J_{net\_2+} \\
J_{net\_2-} \\
J_{net\_3+} \\
J_{net\_3-} \\
J_{net\_4+} \\
J_{net\_4-}
\end{bmatrix} = \begin{bmatrix}
\sigma T_H^4 \\
\sigma\varepsilon_1 T_1^4\alpha \\
\sigma\varepsilon_1 T_1^4\alpha \\
\sigma\varepsilon_2 T_2^4\alpha \\
\sigma\varepsilon_2 T_2^4\alpha \\
\sigma\varepsilon_3 T_3^4\alpha \\
\sigma\varepsilon_3 T_3^4\alpha \\
\sigma T_C^4
\end{bmatrix} \quad \text{(Eq.5)}$$

in terms of the given emissivity values $\varepsilon_{1\text{-}3}$, absolute temperature of the thermal plates $T_{1\text{-}3}$, temperature of the hot collimator space T_H, temperature of the cold optical system space T_C, and the obscuration ratio of the thermal plate α. The effective solid angle Ω_{eff1} and Ω_{eff2} were given in Eq. (3) and (4).

By solving Eq. (5) using an inverse matrix calculation, the net emissive power J values are determined. The thermal loads to the optical system space ΔJ_C and the collimator space ΔJ_H are given as

$$\Delta J_C = J_{net\_4+} - J_{net\_4-} \quad \text{(Eq. 6)}$$

$$\Delta J_H = J_{net\_1-} - J_{net\_1+} \quad \text{(Eq. 7)}$$

where $J_{net\_1\pm}$ and $J_{net\_4\pm}$ are depicted in Fig. 3. A positive thermal load means incoming thermal energy to the space, and a negative value means outgoing thermal energy from the space. The thermal flux for each space can be solved by numerically inverting the matrix in Eq. 5. This was performed for the case listed below in Table 2.

Table 2. Parameters of a thermal sieve

Parameters	Symbol	Value
Diameter of a hole	D_{hole}	0.002 m
Interval between holes	I	0.02 m
Spacing between plates	S	0.25 m
Number of thermal plates	N	3
Wavelength	λ	1μm

The resulting model allows direct evaluation of the thermal performance, as shown in Fig. 4. It is clear that the warm and cold plates (1 and 3) should be highly emissive. The intermediate plate should be highly reflective. The overall performance has strong dependency on the temperature of this plate.
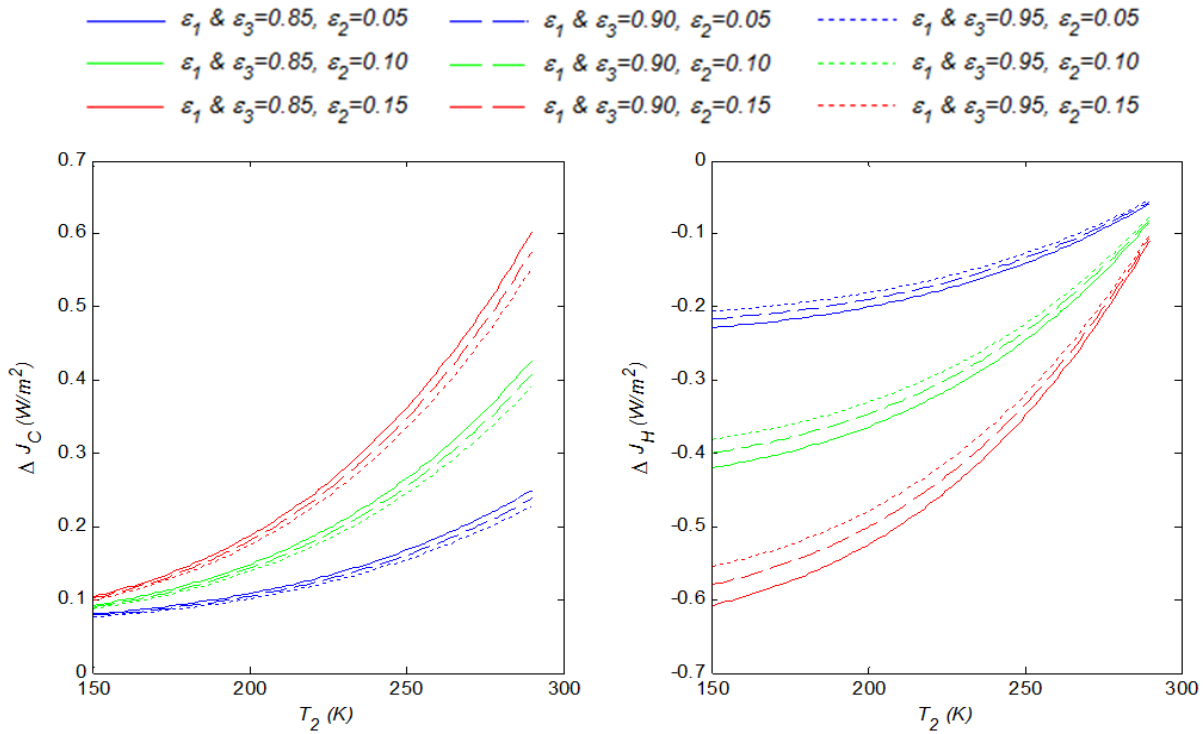
Figure 4. Thermal loads for the cold space (ΔJ_C) and the warm space (ΔJ_H) ambient as a function of the 2nd (middle) thermal plate's temperature T_2 for various emissivity values of the thermal plates (Note: T_1=300K and T_3=35K case).

Figure 4 shows the effect of controlling the temperature of plate 2. A more practical solution would be to allow plate 2 to come to equilibrium at its natural steady state temperature. By applying thermal energy balance for plate 2, we solve for its temperature. This of course depends on the other plates, and is shown in Figure 5. Following this case where the temperature of the middle plate is allowed to float, we evaluate the thermal loading in Figure 6.
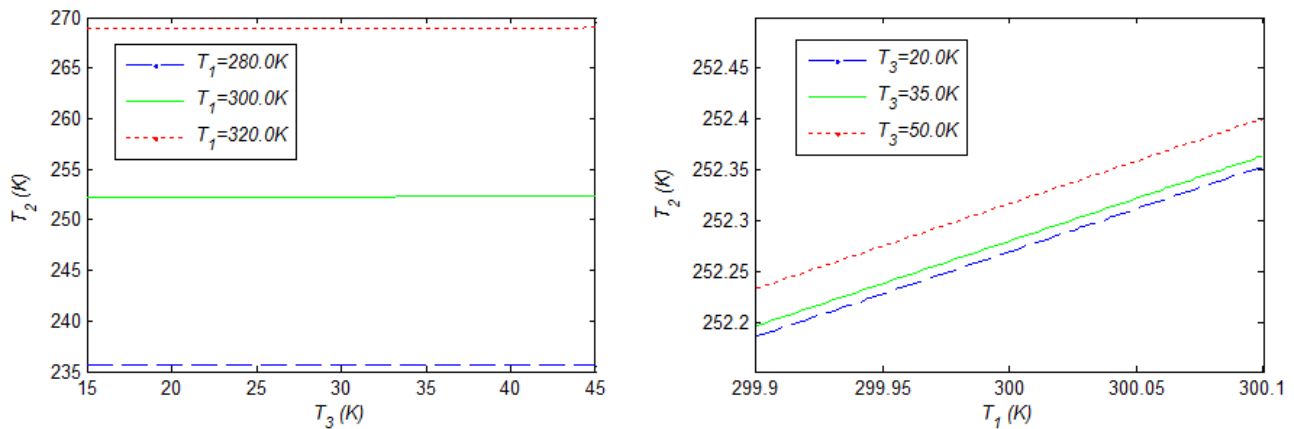
Figure 5. Thermal equilibrium temperature when the 2nd thermal plate is allowed to come to equilibrium: T_2 vs. T_3 (left) and T_1 (right) (Note: ε_1=ε_3=0.9, ε_2=0.1).
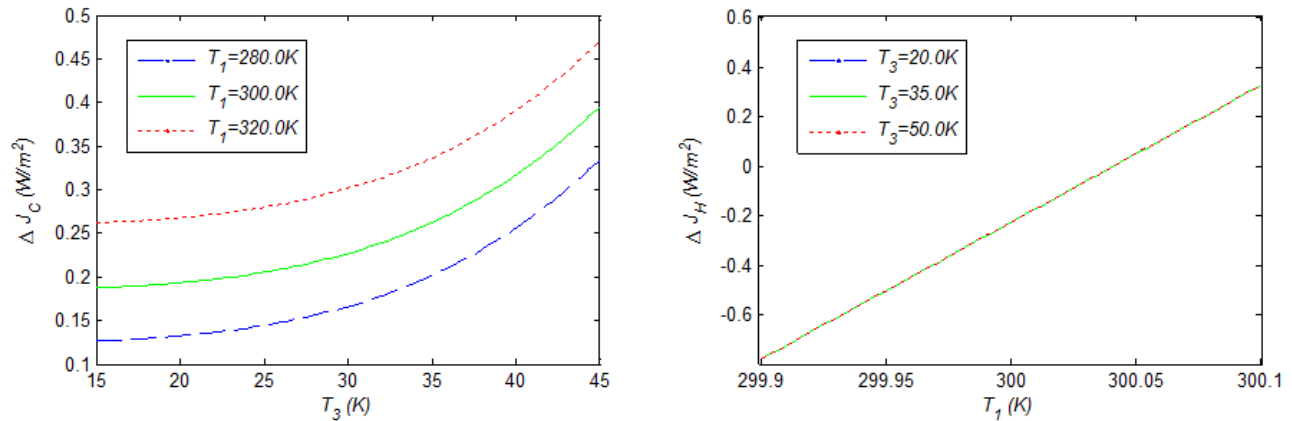
Figure 6. Thermal analysis of system with T_2 allowed to float: Thermal loads to the cold optical system space ΔJ_C (left) and the hot collimator space ΔJ_H (right) (Note: $\varepsilon_1=\varepsilon_3=0.9$, $\varepsilon_2=0.1$).

The thermal modeling was verified with an independent numerical simulation using the Zemax non-sequential ray tracing program. The Zemax model was configured in a way that each surface emits, absorbs, reflects, or scatters rays according to the appropriate temperature and emissivity. The results, shown below in Figure 7, provide corroboration in the thermal model.
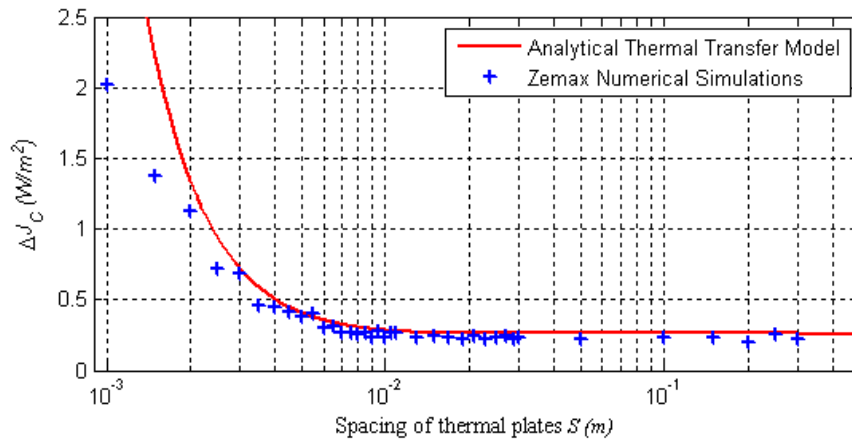
Figure 7. Comparison between the analytical thermal transfer model and Zemax numerical simulations using non-sequential ray tracing (for $T_1=300K$, $T_2=252K$, $T_3=35K$ and $\varepsilon_1=\varepsilon_3=0.9$, $\varepsilon_2=0.1$ case).

3. ANALYSIS OF OPTICAL PERFORMANCE

The thermal sieve blocks the radiative transfer, but allows collimated light to pass as long as the holes are aligned with the geometric propagation of the light. But a diffraction effect due to misalignments can create aberrations in the collimated light. These are evaluated below, for the case of 1μm wavelength and a thermal sieve made of 3 plates with 2 mm holes, 20 mm hole spacing, and 250 mm plate separation.

A diffraction model was constructed to evaluate the propagation of the light as it goes though the holes. The intensity of the light as it passes through the series of ideal holes is shown in Figure 8. The diffraction effects are more interesting when the holes are not perfectly aligned, or have irregular sizes. The effect of these variations causes the diffracted light to have slightly different mean complex amplitude, which will appear as aberrations in the final imaging system.

	Normalized intensity map at thermal plate #			Scale
	1	2	3	
Right before the hole				
Right after the hole				
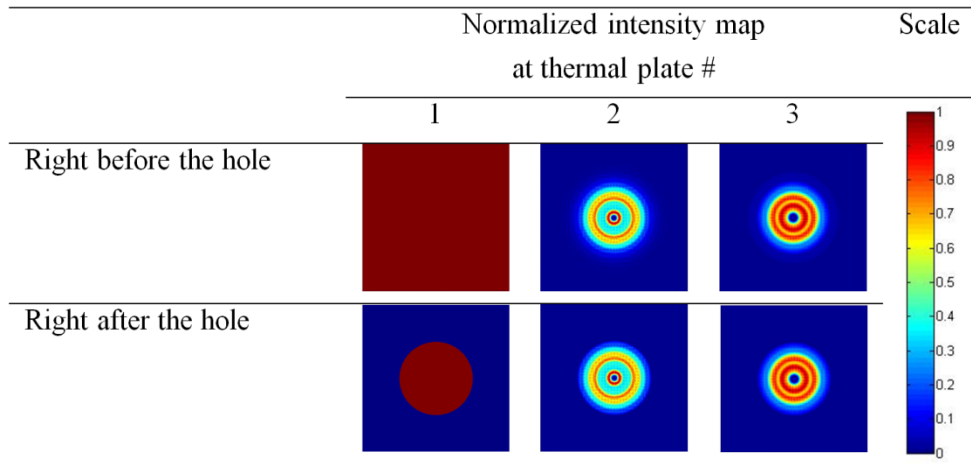
Figure 8. As the light propagates, the diffraction from one hole interacts with the next. This is modeled for ideal holes on thin plate.

.

	Perfect case	Perturbed case
Normalized amplitude map		
Normalized phase map		
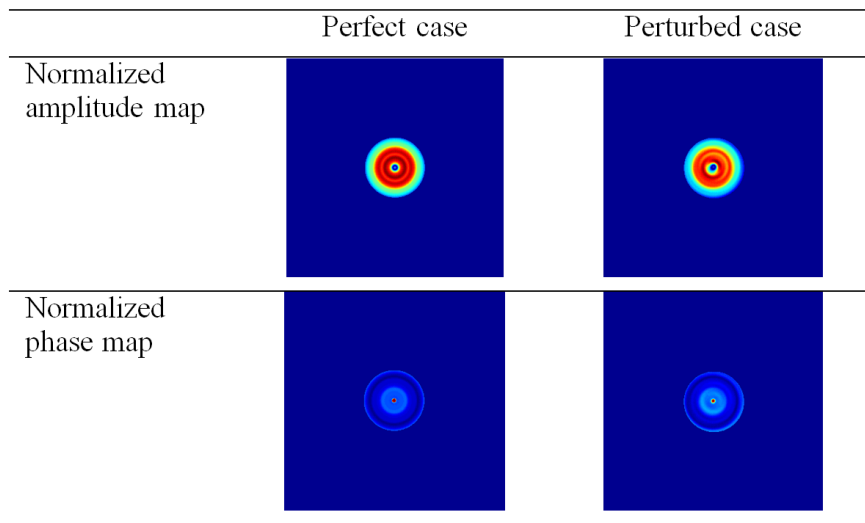
Figure 9. The complex amplitude of the light as it exits the hole in plate 3 will have some amplitude and phase variations due to non-ideal holes. The amplitude and phase are compared for an ideal case, and for a system with 70 µm hole shift and 20 µm diameter variation.

The amplitude and phase of the wavefront that constructs the final image in the system under test is defined by the amplitude and phase of the light as is exits the hole in the last plate. Variations in amplitude are benign, and can be easily calibrated. Variations in phase appear as optical aberrations, and limit the accuracy of the test. A Monte Carlol analysis was performed to investigate the sensitivities. The results, shown in Figure 10, demonstrate that tolerances > 100 µm can be used, yet the diffraction effects will degrade the system wavefront phase by less than 0.003 waves rms.
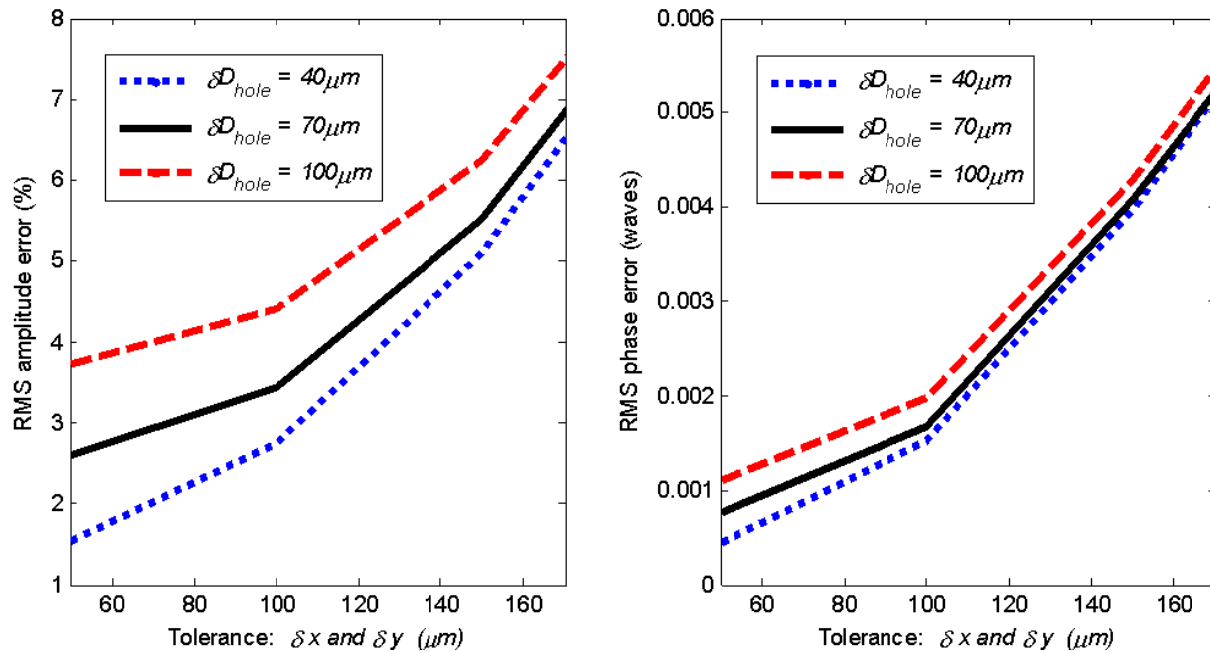
Figure 10. Variations in hole size and placement have an effect on the amplitude and phase of the zero-order light that is used for calibration. The sensitivities shown here are for 2 mm holes, 25 cm plate spacing, and 1 μm wavelength. .

4. DISCUSSION

The thermal sieve can provide excellent thermal isolation between a cryogenic optical system and ambient temperature test optics. The thermal leakage for a simple 3-plate system is on the order of 0.25 W/m^2. Yet the transmitted wavefront is virtually unaffected. Even with realistic manufacturing and assembly tolerances, the system is expected to maintain wavefront accuracy of 0.003 waves.

The hole interval and size, and the plate spacing were chosen somewhat arbitrarily for this preliminary study. Future work is required to understand the tradeoffs and to optimize these parameters for some specific test conditions. Continued work is required to build and assess a practical thermal sieve. The interface issues for the plates, especially at the edges, require development of a testbed to test the ideas and to quantify the manufacturing tradeoffs.

REFERENCES

1) R. Brown and D. Chaney, "Optomechanical tests and performance results of the SIRTF cryogenic optical system," Proc. SPIE **4198** (2001).

2) Barto, A.A., *et al.*, "Optical performance verification of the James Webb Space Telescope", Proc. SPIE 7010, (2008).

3) S. C. West, S. H. Bailey, J. H. Burge, B. Cuerden, J. Hagen, H. M. Martin, and M. T. Tuell, "Wavefront control of the Large Optics Test and Integration Site (LOTIS) 6.5m Collimator," Appl. Opt. **49**, 3522-3537 (2010).

4) D. Kim, W. Cai, and J. H. Burge, "Use of thermal sieve to allow optical testing of cryogenic optical systems," Opt. Express **20**, 12378-12392 (2012).